

# Energy compensation of slow extracted beams with RF acceleration

(加速を伴う遅い取り出しビームのエネルギー変動補正)

指導教員 取越 正己 教授

平成 28 年 2 月

群馬大学大学院医学系研究科

重粒子線医工学グローバルリーダー養成プログラム

平成 24 年入学

重粒子線医学物理・生物学

藤本 哲也

Title: Energy compensation of slow extracted beams with RF acceleration

Tetsuya Fujimoto<sup>a,\*</sup>, Hikaru Souda<sup>a</sup>, Masami Torikoshi<sup>a</sup>, Tatsuaki Kanai<sup>a</sup>, Satoru Yamada<sup>a</sup>, Koji Noda<sup>b</sup>

<sup>a</sup>Gunma University, 3-39-22, Showa, Maebashi, Gunma 371-8511, Japan

<sup>b</sup>National Institute of Radiological Sciences, 4-9-1 Anagawa, Inage, Chiba 263-8555, Japan

\*Corresponding author. Tel.: +81-43-206-3215; fax: +81-43-251-6623; E-mail address: [t.fujimoto@aec-beam.co.jp](mailto:t.fujimoto@aec-beam.co.jp) (T. Fujimoto)

#### Abstract

In a conventional carbon-ion radiotherapy facility, a carbon-ion beam is typically accelerated up to an optimum energy, slowly extracted from a synchrotron ring by a resonant slow extraction method, and ultimately delivered to a patient through a beam-delivery system. At Japan's Gunma University, a method employing slow-beam extraction along with beam-acceleration has been adopted. This method slightly alters the extracted-beam's energy owing to the acceleration component of the process, which subsequently results in a residual-range variation of approximately 2 mm in water-equivalent length. However, this range variation does not disturb a distal dose distribution with broad-beam methods such as the single beam-wobbling method. With the pencil-beam 3D scanning method, however, such a range variation disturbs a distal dose distribution because the variation is comparable to slice thickness. Therefore, for pencil-beam 3D scanning, an energy compensation method for a slow extracted beam is proposed in this paper. This method can compensate for the aforementioned energy variances by controlling net energy losses through a rotatable energy absorber set fixed between the synchrotron exit channel and the isocenter. Experimental results demonstrate that beam energies can be maintained constant, as originally hypothesized. Moreover, energy-absorber positions were found to be significantly enhanced by optimizing beam optics for reducing beam-size growth by implementation of the multiple-scattering effect option.

Keywords: energy absorber; scanning irradiation; slow extraction

## 1. Introduction

A carbon-ion beam is particularly suitable for deeply seated cancer radiotherapy, owing to its high dose localization potential and high biological effect in the Bragg-peak region. Gunma University's Heavy Ion Medical Center (GHMC) was therefore constructed as a pilot facility for implementing a compact carbon-ion radiotherapy unit in Japan [1]. The GHMC has been successfully operated since 2010, with more than 1,600 patients having undergone treatment till March 2015 [2]. The facility consists of an injector cascade [3], a synchrotron ring, and four irradiation rooms (three for cancer treatment and one for research). The research room is utilized for physics- and biological-related experiments; moreover, pencil-beam 3D scanning [4, 5, 6, 7] has been developed for precise radiotherapy via the employment of a sub-millimeter size carbon-ion beam.

The synchrotron can accelerate the carbon-ion beam up to 400 MeV/u with a betatron tune of  $(Q_x, Q_y) = (1.68, 1.23)$ . Accelerated carbon ions are extracted from the synchrotron by a third-order resonant slow-extraction beam acceleration method [8, 9]. In this method, the beam is accelerated to bring the horizontal betatron tune,  $Q_x$ , close to a third-order resonance of  $5/3$ . Applying Hardt's condition, this method can extract ions with different momenta along the same outgoing separatrix independent of each momentum while the momenta vary depending upon the radio frequency (RF) of the acceleration. The momentum variation in present operations is 0.3%, corresponding to 2.0 mm and 1.6 mm in water-equivalent length (WEL) at 400 MeV/u and 290 MeV/u, respectively. The extent of this range variation does not disturb the distal dose distribution in the case of a broad-beam irradiation method [10] because the variation is averaged owing to a much faster wobbling speed compared with that of the momentum variation. However, for a spot/raster scanning irradiation method, this momentum variation disturbs the distal dose distribution because the irradiation time on each spot is much faster than that of the momentum variation. In such a case, uniformity of the irradiation field worsens because the averaging effect for the broad-beam irradiation method is not anticipated. Thus, for the present slow-extraction method, an energy-compensation mechanism has been strongly required for realizing effective pencil-beam 3D scanning irradiation at GHMC. One implemented solution is beam acceleration or deceleration in a beam-transport line between a synchrotron exit and an isocenter. This method cannot, however, suppress energy variations using an electric field because of the fact that it requires a high voltage of 5.2 MV to generate an initial beam energy of 400 MeV/u with a charge-to-mass ratio of  $1/2$ . Therefore, we propose the use of an energy absorber for keeping the beam energy constant. The experimental results verified that the proposed method can maintain a constant beam energy even when varying the beam energy from the synchrotron during the extraction period.

In the pencil-beam 3D scanning process, the beam-size variation relative to the isocenter should be minimized independent of varying effective thickness of the absorber during extraction. For this purpose, an optimization method for beam optics is proposed and evaluated in this study.

## 2. The energy absorber method

### 2.1 Principle

For applying the slow-extracted beam with the beam-acceleration method to actual radiotherapy scenarios, it is important to reduce momentum variation to the lowest extent possible. To reduce the momentum variation of the extracted beam and to reduce the space-charge effect during the injection period, the beam is injected into the synchrotron through a multi-turn injection process, leading to a hollow distribution of horizontal phase space at the GHMC. Turn numbers of the multi-turn injection are determined for obtaining a beam intensity of  $2 \times 10^9$  pps, which is a necessary intensity for attaining a sufficient irradiation dose. To extract all accumulated ions via the beam-acceleration method, a momentum variation of the slow-extracted beam is estimated at 0.3% under a horizontal chromaticity of  $\xi_x = -1.1$ , which can be controlled by adjusting the sextupole fields for chromaticity correction. The separatrices with a central momentum of 0.0% and 0.3% are shown in Fig. 1. Figs. 2 (A) and (B) show the energy variation in one operational period of the synchrotron and an enlarged view of the beam extraction period in the case of 400 MeV/u, respectively. This energy variation can be calculated from the acceleration RF frequency of the synchrotron. The beam energy gradually increases from 400 MeV/u to 402.6 MeV/u during beam extraction, and all ions are extracted from the synchrotron owing to negative horizontal chromaticity.

The principle of the proposed energy-absorber method is as follows: We can keep the energy constant by varying the energy loss, which can be calculated by Bethe–Bloch formula [11], according to the extent of beam-energy variation during extraction. It is noted that the energy loss is caused by the energy absorber set in the beam transport line. To obtain constant beam energy during the extraction period by using the energy absorber, it is necessary to control the overall amount of energy loss. Therefore, we devised a rotating absorber structure to change the effective thickness of the absorber. The energy loss can then be easily varied by changing its effective thickness by rotating the absorber. A major advantage of using the rotating structure is the compensation of energy variation with a high degree of accuracy; it is noted, however, that the beam energy does not constantly vary because the structure can continuously and easily adjust absorber thickness. Furthermore, the same absorber can be used for all beam energies ranging from 400 MeV/u to 140 MeV/u by changing the rotation angle. Assuming that aluminum is used as the absorber material, an absorber thickness of 1 mm is necessary when the maximum rotation angle is limited to less than  $65^\circ$  (to maintain an aperture). Table 1 presents potential rotation angles calculated under various initial energies.

### 2.2 Experiment

#### 2.2.1. Experimental setup

Energy compensation is verified during the entire extraction period by measuring Bragg peak positions as opposed to the greater challenges associated with direct beam energy measurements. Fig. 3

presents the experimental setup. A water tank (in which the depth of water can be varied) and a parallel-plate-type ion chamber (with a large window) were set up at the isocenter to measure the Bragg peak. Ion numbers from the accelerator were measured with a dose monitor that is located at the exit of the irradiation port 1.5 m upstream from the isocenter. A pencil beam with a beam size of  $2.2 \text{ mm}$  in  $1\sigma$  was irradiated through the center of the dose monitor and energy absorber to the isocenter with a position deviation of less than  $0.2 \text{ mm}$ . The Bragg peak position was derived from the current signal ratio of the ion chamber to the dose monitor. The energy absorber was set at  $0.75 \text{ m}$  upstream of the isocenter, and the motion of the energy absorber was controlled by a servomotor. In this experiment,  $1 \text{ mm}$ -thick aluminum was selected as the absorber material. All accelerator complex devices were operated by a master trigger. Therefore, we controlled the motion of the absorber using the master trigger. The absorber rotation angle was calculated from the RF frequency pattern of the synchrotron and the angle data were written into a programmable logic controller.

### 2.2.2 Experimental results

The energy absorber experiment was conducted with a beam energy of  $290 \text{ MeV/u}$ . According to calculations, the Bragg-peak position shifts by  $1.6 \text{ mm}$  for this energy. We measured Bragg peaks with delay times from master triggers of  $790$ ,  $1,250$ , and  $1,715 \text{ ms}$ , which correspond to the beginning, middle, and end of the extraction section, respectively. To measure the Bragg-peak position accurately, the water depth was varied at  $0.2 \text{ mm}$  steps. Fig. 4 (A) shows the measured Bragg peak via an ordinary beam. The Bragg peak position shifted with time evolution, with a shift of  $1.5 \text{ mm}$  being observed during an extraction period of  $1 \text{ second}$ . This result was in good agreement with corresponding calculations. From the Bragg peaks with the energy absorber (Fig. 4 (B)), it was verified that the energy absorber method maintained the Bragg peak positions constant, which correspond to the various beam energies from the synchrotron. This result shows that energy compensation was realized throughout the entire extraction section.

### 3. Transverse motion

To utilize the energy absorber for scanning irradiation scenarios, it is important to keep the beam size as small as possible at the isocenter. When charged particles pass through matter, there exists not only energy loss but also considerable scattering. Therefore, an emittance growth occurs after passage through the energy absorber. Furthermore, such a growth increases systematically because the thickness of the energy absorber is constantly varied during the extraction period. This emittance growth naturally results in a corresponding beam-size growth. Hence, we scrutinized an ideal setting position and beam-line optics for maintaining the beam condition at the isocenter.

Assuming that the energy absorber is very thin, a particle remains at the same transverse position when passing through the absorber. It means that the beam size does not vary just in front of or just

behind the absorber. In this case, the relation of beam emittance ( $\varepsilon$ ) just in front of and just behind the energy absorber is shown as eq. (1) [12].

$$\varepsilon_2 = \varepsilon_1 \sqrt{1 + \frac{\beta_1 \theta_0^2}{\varepsilon_1}}, \quad (1)$$

where  $\theta_0$  is the scattering angle, and subscripts 1 and 2 depict beam emittance values just in front of and just behind the absorber, respectively. The scattering angle can be calculated from Highland's equation [13]; from this equation it is obvious that emittance growth reduces by minimizing the  $\beta$ -function at the energy absorber.

On the other hand, with regard to maintaining the beam size, the relation of beam size between the isocenter and the absorber is expressed as follows:

$$\begin{pmatrix} \varepsilon_2 \beta_i \\ \varepsilon_2 \alpha_i \\ \varepsilon_2 \gamma_i \end{pmatrix} = \begin{pmatrix} m_{11}^2 & -2m_{11}m_{12} & m_{12}^2 \\ -m_{21}m_{11} & 1 + 2m_{12}m_{21} & -m_{12}m_{22} \\ m_{21}^2 & -2m_{22}m_{21} & m_{22}^2 \end{pmatrix} \begin{pmatrix} \varepsilon_2 \beta_2 \\ \varepsilon_2 \alpha_2 \\ \varepsilon_2 \gamma_2 \end{pmatrix}, \quad (2)$$

where subscripts 2 and  $i$  of the Twiss parameters appear just behind the absorber and the isocenter, respectively. Furthermore,  $m$  depicts the elements of the transfer matrix from the absorber to the isocenter. From this matrix, the square of the beam size at the isocenter is expressed as follows:

$$\varepsilon_2 \beta_i = m_{11}^2 \varepsilon_2 \beta_2 - 2m_{11}m_{12} \varepsilon_2 \alpha_2 + m_{12}^2 \varepsilon_2 \gamma_2. \quad (3)$$

When a thin absorber is used, the beam size just behind the absorber (root of  $\varepsilon_2 \beta_2$ ) is kept constant regardless of absorber thickness. To keep the beam size at the isocenter constant for any absorber thickness, it is necessary to find the condition at which eq. (3) results in a fixed value. To realize this condition, the following two essential conditions must be satisfied: (1) the first term has to be a constant value (namely,  $m_{11}$  has to be a fixed value) and (2) the second and third terms have to be zero because  $\alpha_2$  and  $\gamma_2$  vary during the beam extraction period with the absorber thickness. Therefore,  $m_{12}$ , which is the common element of the second and third term, has to be zero. Each element of the transfer matrix, from the absorber to the isocenter, is expressed through Twiss parameters as follows:

$$\begin{aligned}
m_{11} &= \sqrt{\frac{\beta_{i0}}{\beta_{20}}} (\cos \mu + \alpha_{20} \sin \mu), \\
m_{12} &= \sqrt{\beta_{20} \beta_{i0}} (\sin \mu), \\
m_{21} &= -\sqrt{\frac{1}{\beta_{20} \beta_{i0}}} ((\alpha_{i0} - \alpha_{20}) \cos \mu + (1 + \alpha_{i0} \alpha_{20}) \sin \mu), \text{ and} \quad (4) \\
m_{22} &= \sqrt{\frac{\beta_{20}}{\beta_{i0}}} (\cos \mu - \alpha_{i0} \sin \mu),
\end{aligned}$$

Where  $\mu$  is the betatron phase advance and subscripts 20 and  $i0$  show the initial Twiss parameters at the energy absorber and the isocenter, respectively, which are calculated when the absorber angle is equal to zero. It is obvious that the above two conditions are satisfied under the baseline condition of  $\mu = (\text{integer}) \times \pi$ . At any point with a phase advance an  $(\text{integer}) \times \pi$  from the absorber, the position of a beam particle is independent of its angle at the absorber. Therefore, the isocenter beam size is kept constant, and defined as follows:

$$\sqrt{\varepsilon_2 \beta_i} = \sqrt{\frac{\beta_{i0}}{\beta_{20}}} \times \sqrt{\varepsilon_2 \beta_2}. \quad (5)$$

Fundamentally, the beam size at the isocenter will not vary even if the scattering angle gradually varies. Accordingly, we investigated whether the execution of optimized beam optics is altogether possible at the GHMC facility. In addition, we considered optics with  $\alpha = 0$  at the isocenter, which is a necessary and sufficient condition for scanning irradiation scenarios. As a result of this investigation, an ideal setting position of the absorber and optimized optics for the beam transport line were determined that satisfactorily fulfill the above conditions. Horizontal and vertical beta functions of 1.6 m and 0.75 m were realized at the absorber, respectively. With these beta functions, emittance after passage through the absorber of 1 mm thickness vary from 0.25 to 0.60  $\pi$  mm $\cdot$ mrad at horizontal and from 0.50 to 0.92 $\pi$  mm $\cdot$ mrad at vertical.

Table 2 shows the calculated parameters at the isocenter by using optimized transport line optics. The beam size at the isocenter is kept constant during extraction. Fig. 5 shows the beam envelope from an electrostatic septum deflector to the isocenter of the scanning irradiation room via optimized optics. After passing through the absorber, the beam size expands proportional to the absorber thickness with the progression of emittance growth over time. However, it is acceptable for our beam transport line.

## 5. Summary

In support of evaluating 3D scanning irradiation scenarios at GHMC, this study considered the use of an energy absorber medium to obtain a constant beam energy level. Energy variation, which is caused by

the slow extraction method with RF sweeping, is estimated at 0.67% at 400 MeV/u and 0.70% at 290 MeV/u. To correct this energy variation, we integrated a rotating structure configuration to the energy absorber. Experimental results ultimately confirmed that a constant beam energy is indeed achieved via the use of an energy absorber.

On the other hand, when utilizing such an energy absorber for scanning irradiation purposes, it is important to maintain a beam size that is small and constant at the isocenter. We determined a suitable condition that keeps the beam size constant in the beam transport line. From these results, it was concluded that the GHMC will be able to consistently supply a high quality beam, which can thus be utilized for a host of scanning irradiation applications.

The proposed method is independent on the ion species. Therefore, it would be effective for the proton facilities, which are adopting the same slow extraction method with our facility.

#### Acknowledgement

The authors would like to express their appreciation to Prof. Nakano and Prof. Ohno of the Gunma University's Graduate School of Medicine for their significant input and useful advice and to members of the GHMC operations team for their skillful applications. This study was conducted as part of a program for cultivating global readers on heavy ion therapeutics and engineering at Gunma University.

#### Reference

- [1] K. Noda, T. Furukawa, T. Fujisawa, Y. Iwata, T. Kanai, M. Kanazawa, A. Kitagawa, M. Komori, S. Minohara, T. Murakami, M. Muramatsu, S. Satou, Y. Takei, M. Tashiro, M. Torikoshi, S. Yamada, K. Yusa, *New Accelerator Facility for Carbon-Ion Cancer-Therapy*, *J. Radi. Res.*, 48 (2007) A43-A54.
- [2] T. Ohno, T. Kanai, S. Yamada, K. Yusa, M. Tashiro, H. Shimada, K. Torikai, Y. Yoshida, Y. Kitada, H. Katoh, T. Ishii, T. Nakano, *Cancers* 3, 4046-4060 (2011)
- [3] Y. Iwata, S. Yamada, T. Murakami, T. Fujimoto, T. Fujisawa, H. Ogawa, N. Miyahara, K. Yamamoto, S. Hojo, Y. Sakamoto, M. Muramatsu, T. Takeuchi, T. Mitsumoto, H. Tsutsui, T. Watanabe, T. Ueda, *Performance of a compact injector for heavy-ion medical accelerators*, *Nucl. Instrum. Meth. A* 572 (2007) 1007-1021.
- [4] T. Kanai, K. Kawachi, H. Matsuzawa, T. Inada, *Nucl. Instrum. Methods Phys. Res.* 214 (1983) 491-496.
- [5] Th. Haberer, W. Becher, D. Schardt, G. Kraft, *Nucl. Instr. and Meth. A* 330 (1993) 296.
- [6] T. Furukawa, T. Inaniwa, S. Sato, T. Shirai, Y. Takei, E. Takeshita, K. Mizushima, Y. Iwata, T. Himukai, S. Mori, S. Fukuda, S. Minohara, E. Takada, T. Murakami, K. Noda, *Med. Phys.* 37 (2010) 5682-5682.
- [7] T. Kanai, K. Kawachi, Y. Kumamoto, H. Ogawa, T. Yamada, H. Matsuzawa, T. Inada, *Med. Phys.* 7



(1980) 365

- [8] W. Hardt, LEAR Note 79-4 (1979)
- [9] W. Hardt, LEAR Note 81-6 (1981)
- [10] W. T. Chu, B. A. Ludewigh, T. R. Renner, Rev. Sci. Instr. 64, 2055-2122 (1993)
- [11] H. A. Bethe, Phys. Rev. 89 (1953)
- [12] A. Maier, CERN/PS 98-061 (DI)
- [13] V. L. Highland, Nucl. Instr. and Meth. 129 (1975) 497-499.

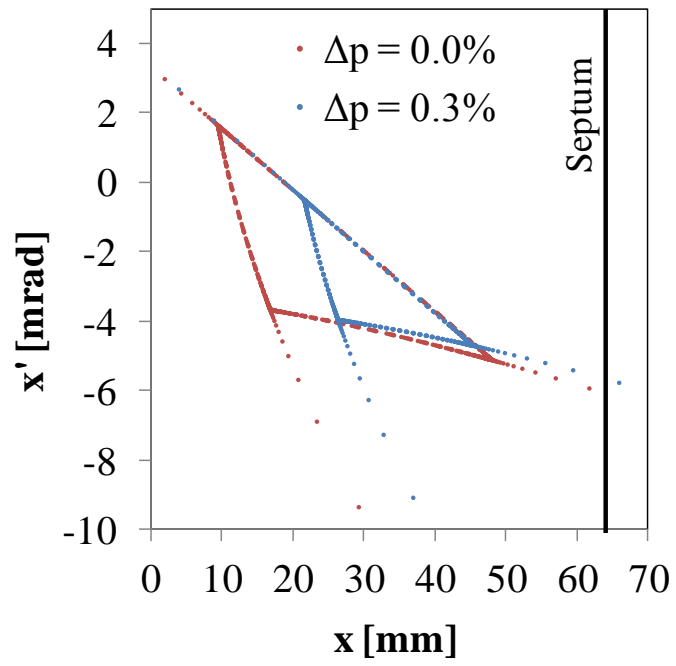


Fig. 1. Transition of separatrix size and position with  $\Delta p = 0.0\%$  and  $0.3\%$ .

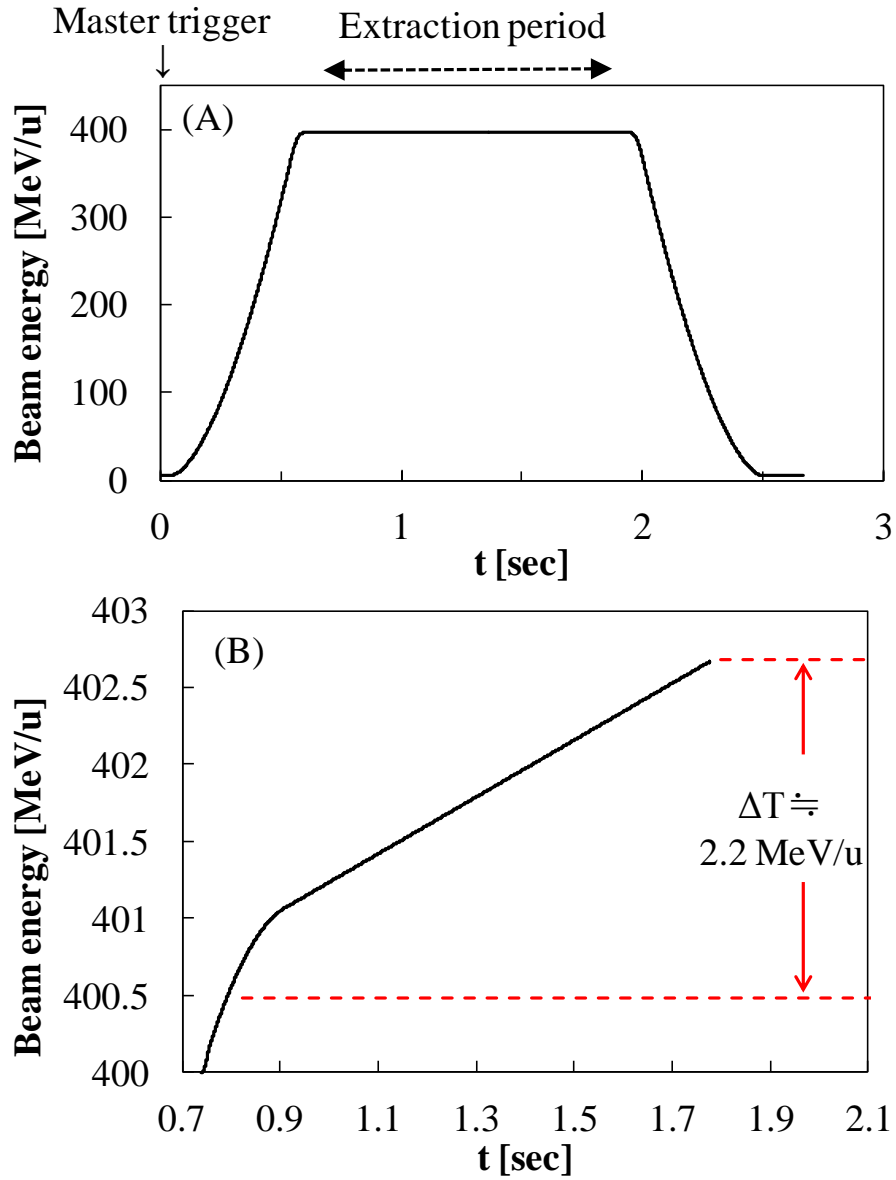


Fig. 2. Energy variation in the extraction period in the case of 400 MeV/u. (A) Operation pattern of the synchrotron, which is repeated every 3 s. (B) Enlarged view of the extraction period. Carbon ions are extracted within the dotted lines in figure (B).

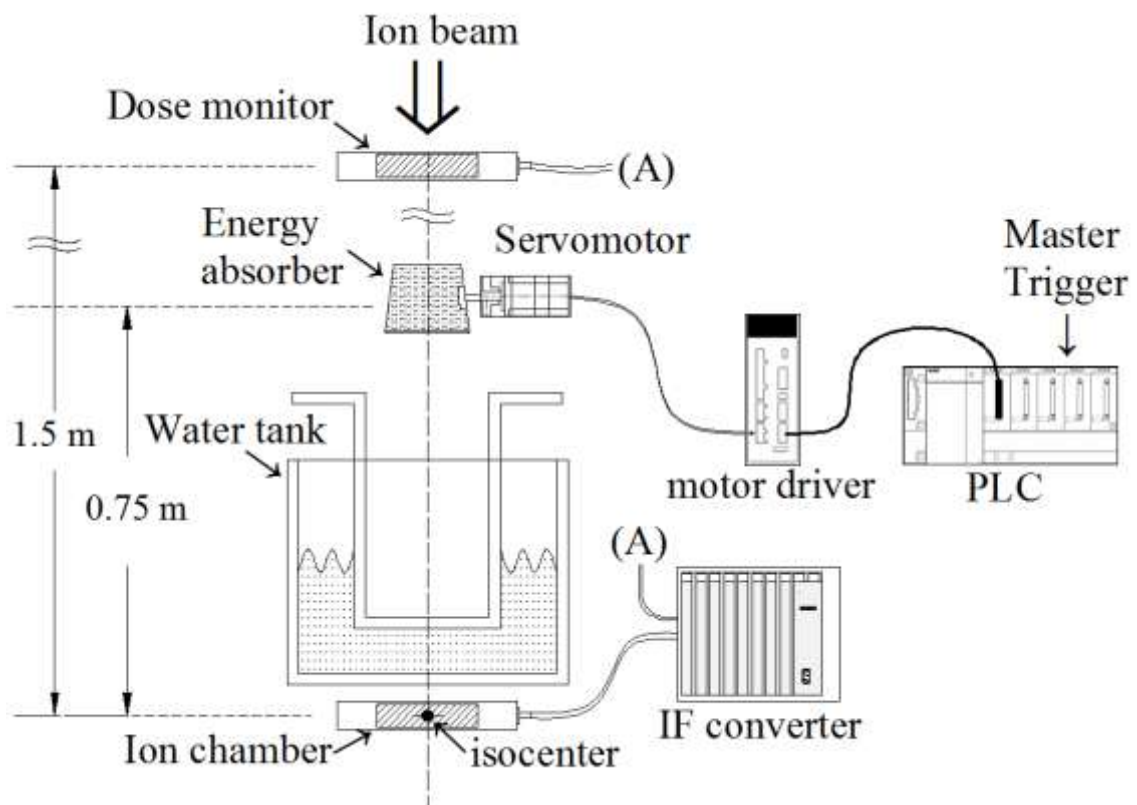


Fig. 3. Experimental setup for energy compensation by using an energy absorber.

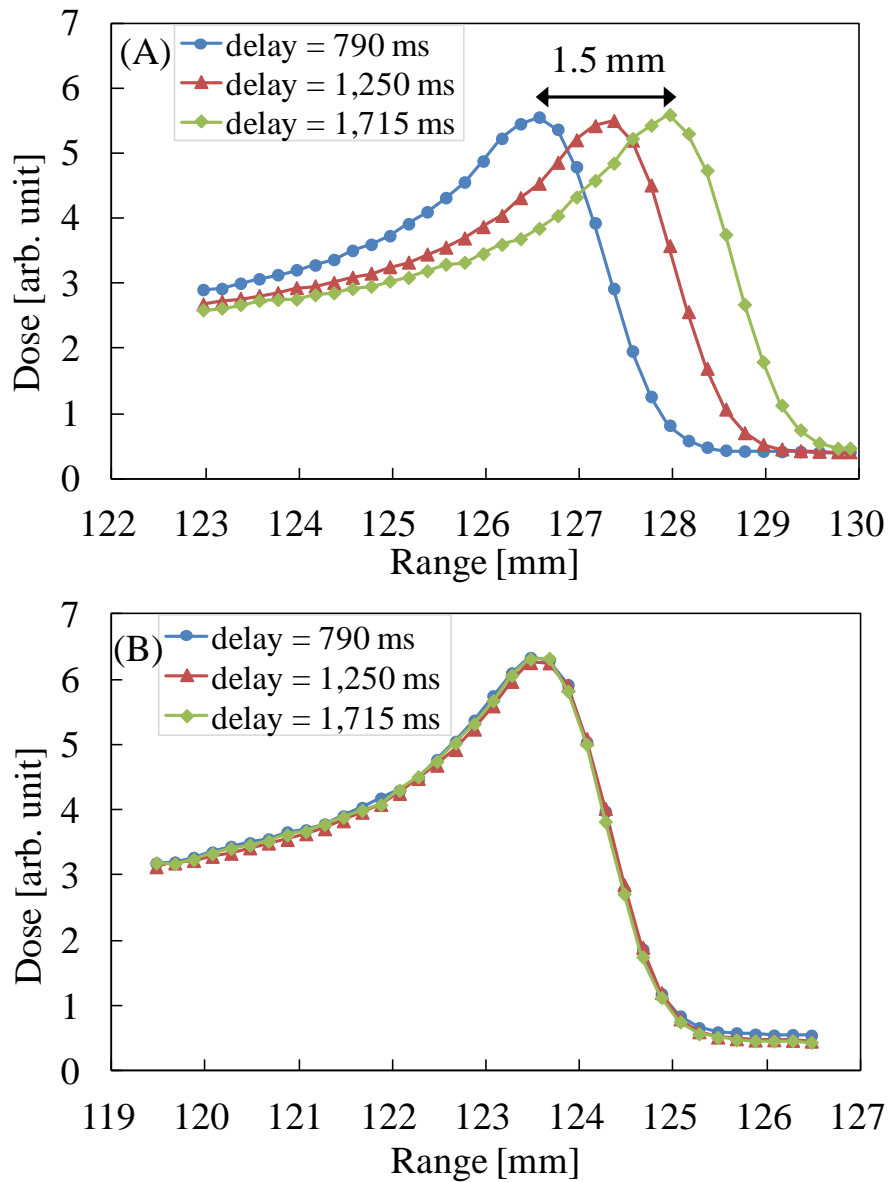


Fig. 4. Experimental results of energy compensation tests. The horizontal axis shows the depth of water, which corresponds to the range, and the vertical axis shows the measured dose. Bragg peaks were measured at delay times from a master trigger of 790, 1,250, and 1,715 ms. These delays correspond to the beginning, middle, and end of the extraction period, respectively. (A) Results via an ordinary beam, and (B) results with an energy absorber.

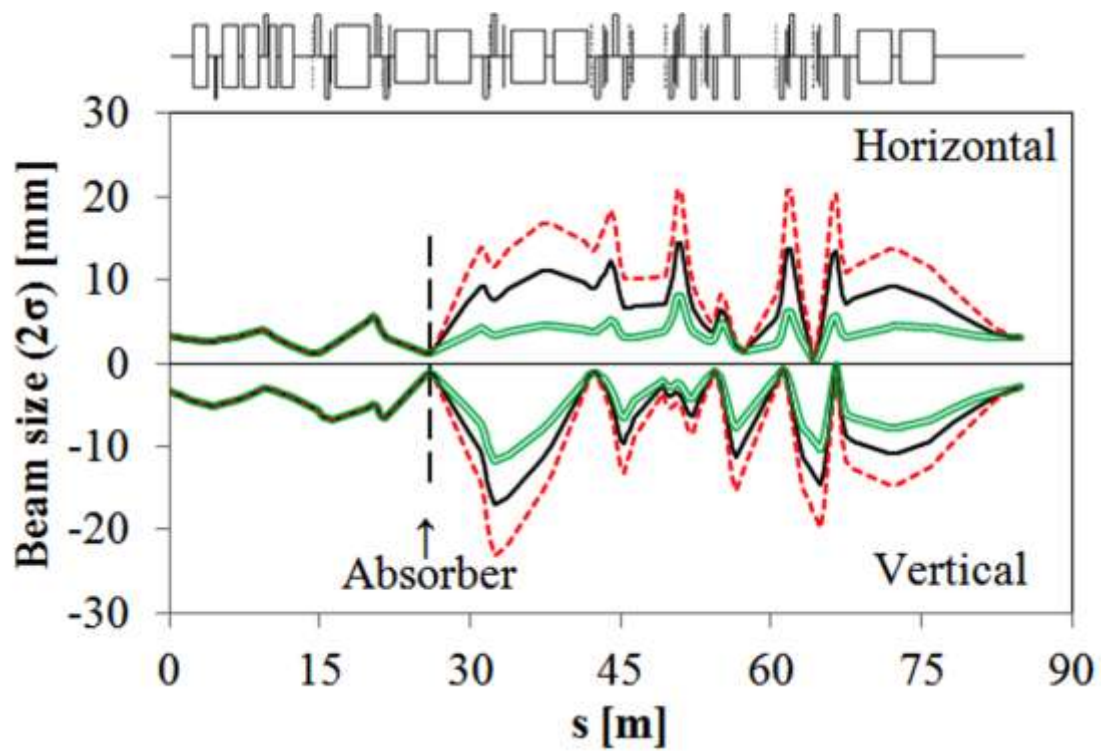


Fig. 5. Beam envelope from the electrostatic septum deflector to the isocenter of the scanning research room. The double line shows the envelope without absorber and the solid lines and dotted lines show the envelope with absorber thicknesses of 1 mm and 2.38 mm, respectively.

Table 1

Rotation angle of the energy absorber using aluminum of 1 mm thickness.

Beam energy (MeV/u)	400 → 402.68	290 → 292.02	140 → 141.05
Absorber thickness (mm)	1 → 2.38	1 → 1.88	1 → 1.28
Rotation angle (degree)	0 → 65	1 → 57.9	1 → 38.6
Corrected Beam energy (MeV/u)	398	287.7	136.3

Table 2

Calculated parameters at the isocenter by using optimized optics.

	Beginning	End
Beam energy (MeV/u)	400	402.68
Absorber thickness (mm)	1	2.38
$\epsilon_x$ at $1\sigma$ ( $\pi\text{mm}\cdot\text{mrad}$ )	0.602	0.92
$\epsilon_y$ at $1\sigma$ ( $\pi\text{mm}\cdot\text{mrad}$ )	0.729	0.9915
$\beta_x$ at isocenter (m)	3.64	2.38
$\beta_y$ at isocenter (m)	2.98	2.21
Beam size $2\sigma_x$ (mm)	3.0	3.0
Beam size $2\sigma_y$ (mm)	3.0	3.0
Energy spread (%)	0.101	0.102